Results in Engineering 32 (2026) 111900

Contents lists available at ScienceDirect

Results in Engineering

journal homepage: www.sciencedirect.com/journal/results-in-engineering

Research paper

Integrating water pinch analysis and GIS for optimized industrial cluster water reuse: A case study of the port of Amsterdam

C.J. Teo [a,b,*], J. Poinapen [a], J.A.M.H. Hofman [c], T. Wintgens [b]

[a] KWR Water Research Institute, Water Treatment & Resource Recovery, Groningenhaven 7, 1072 3430 BB, Nieuwegein, Utrecht, The Netherlands
[b] Institute of Environmental Engineering, RWTH Aachen University, Mies-van-der-Rohe-Strasse 1, D-52074 Aachen, Germany
[c] Department of Chemical Engineering, University of Bath, Bath BA2 7AY, UK

ARTICLE INFO

Keywords:
Water reuse
Water minimisation
Industrial water
Circular economy
Industrial symbiosis

ABSTRACT

This study introduces an integration of Water Pinch Analysis (WPA) and Geographic Information Systems (GIS) to optimize water reuse in industrial clusters, jointly addressing water quality compatibility and spatial constraints. The research analyzed 17 industrial facilities in the Port of Amsterdam to identify water reuse opportunities and reduce freshwater dependency. Using chloride as a single-contaminant proxy to define the scope of all quantitative results in this study, the analysis shows that the maximum freshwater savings, which reduce consumption from 79.2 m^3/h to 10.3 m^3/h would require a pipeline length of 39.4 km. These figures represent a theoretical upper bound under single-contaminant matching conditions. However, scenarios with shorter pipelines, averaging 17.8 km with a median of 14.7 km, achieved less ambitious water savings, illustrating the trade-offs between infrastructure investments and water reuse efficiency. The findings demonstrate that spatially constrained, quality-based reuse planning can significantly reduce freshwater dependency in industrial clusters, with the framework offering a reproducible methodology applicable to eco-industrial parks facing similar water scarcity pressures. This integrated approach provides actionable insights for circular water management in eco-industrial parks and offers a pathway to addressing global water sustainability challenges.

1. Introduction

Water scarcity, driven by increased water demand due to population growth, industrial expansion, and climate change, is a growing global concern. The traditional linear economic model, emphasizing resource extraction, use, and discharge, has long dominated water management. However, increasing awareness of its environmental, economic, and social impacts has driven a global shift toward sustainable practices. Freshwater resources are finite, and their inefficient use has resulted in both significant environmental harm and resource scarcity [1,2]. Consequently, nations are restructuring water systems to address these challenges [3,4].

Industrial water use, accounting for 22% of global freshwater consumption, further strains these resources [5,6]. Moreover, the competition between domestic, industrial and agricultural sectors is intensifying due to increasing population and industrial growth, as global water demand is projected to exceed supply by 40% by 2030, necessitating efficient allocation and reuse strategies. A circular approach, where treated wastewater is reused within industrial processes, can significantly reduce both freshwater demand and wastewater production [7–9]. By incorporating resource-efficient designs, industries can enhance water sustainability while reducing operational cost [10].

Water Pinch Analysis (WPA) has been widely applied in optimizing water reuse in industrial processes. Inspired by Mass Exchange Networks (MEN), WPA identifies opportunities to minimize freshwater consumption by matching water demand with the quality of available wastewater streams[11,12]. Industrial parks and eco-industrial clusters often require intricate water networks but optimizing water reuse within these networks, which must account for physical infrastructure and geographical constraints to provide opportunities for sustainable initiatives. Existing MEN approaches primarily focus on individual industrial facilities, presenting an opportunity to extend these methodologies to industrial cluster settings with complex spatial dynamics.

To address this gap, this study integrates Geographic Information Systems (GIS) into Water Pinch Analysis, providing a spatial dimension to aid water reuse optimization. By incorporating GIS, the spatial layout

* Corresponding author at: KWR Water Research Institute, Water Treatment & Resource Recovery, Groningenhaven 7, 1072 3430 BB, Nieuwegein, Utrecht, The Netherlands.
E-mail address: chuan.jiet.teo@rwth-aachen.de (C.J. Teo).

https://doi.org/10.1016/j.rineng.2026.111900
Received 17 April 2025; Received in revised form 29 June 2026; Accepted 7 July 2026
Available online 8 July 2026
2590-1230/© 2026 The Author(s). Published by Elsevier B.V. This is an open access article under the CC BY license (http://creativecommons.org/licenses/by/4.0/).

of industries, road networks and existing infrastructure can be analyzed, allowing for the design of more efficient and feasible water reuse systems. This approach enhances the applicability of WPA, particularly in large-scale industrial clusters where spatial factors are critical.

The Port of Amsterdam, an eco-industrial park with diverse water needs, serves as the case study for this research. This region is undergoing rapid industrial expansion while facing increasing pressure to reduce freshwater use. The integration of WPA with GIS offers a promising solution for sustainable water management in this context. This study aims to contribute to the development of more comprehensive water distribution and reuse strategies that are refined both in terms of resource efficiency and spatial feasibility, providing valuable insights for industries and policymakers.

2. Background

The development of Mass Exchange Networks (MENs) has been pivotal in optimizing water use in industrial processes. Wang and Smith (1994) introduced a graphical approach to minimize freshwater consumption and wastewater discharge by transferring contaminants between process and water streams[11]. This foundational method was refined by El-Halwagi et al. (2003) and later expanded to include mass transfer operations, emphasizing minimal external stream usage [12, 13]. Olesen and Polley (1997) simplified single contaminant design procedures, enhancing reuse and recycle designs, while Hallale (2002) introduced a graphical targeting method for water minimization. Gomes et al. (2007) contributed the Water Source Diagram (WSD), a heuristic tool for synthesizing water mass exchange networks, underscoring the utility of graphical tools in addressing complex design challenges [14–16]. Practical applications of these methodologies span various industries, with successes reported in ethanol production, starch processing, and oil refining [17–19]. Graphical approaches such as WPA, mathematical programming methods have become pivotal in designing industrial water networks. Techniques such as Linear Programming (LP), Mixed-Integer Linear Programming (MILP), and Nonlinear Programming (NLP) offer superior flexibility in constraint modeling, cost optimization, and integration of treatment systems. For example, Alva-Argáez et al. (2007) introduced a mixed-integer nonlinear programming (MINLP) model for refinery water-using systems, enabling simultaneous consideration of freshwater cost, wastewater treatment, piping cost, and environmental constraints [20]. Additionally, Tan et al. (2007b) developed an approximate MILP superstructure for designing water reuse and recycling networks, achieving up to ~27% freshwater savings and substantial cost reductions [21]. In another stream, Faria & Bagajewicz (2009) presented a mathematical optimization framework for grassroots design and retrofit of water systems, optimizing for net present value (NPV) or return on investment (ROI), rather than just reducing freshwater consumption [22]. These optimization-based methods provide high precision and adaptability, especially in scenarios with multiple contaminants and dynamic operational constraints. In contrast, the present approach combines WPA's heuristic transparency with GIS-driven spatial routing to jointly address water quality matching and physical infrastructure constraints, an integration that, while drawing on established methods in both domains, has received limited empirical evaluation in brownfield industrial cluster settings with heterogeneous water users.

Eco-industrial parks (EIPs) and industrial clusters have been frontrunners for promoting sustainable industrial practices, particularly in water resource management. Lovelady and El-Halwagi (2009) proposed an optimization-based model for EIP design focused on recycling, reuse, and separation processes [23]. While this method successfully demonstrated cost savings, supplementing such frameworks with detailed, spatially explicit quantitative data can further support their broader practical implementation. Similarly, life cycle assessments (LCA) in China have highlighted environmental benefits of water reuse, such as a 20% reduction in greenhouse gas emissions [24]. However, applying these findings to diverse industrial contexts requires careful consideration of local conditions which can significantly alter outcomes. Taskhiri et al. (2011) introduced an energy-based fuzzy optimization model for EIPs, claiming up to 30% cost savings [25]. However, approaches utilizing fuzzy logic to balance sustainability and economic goals often involve qualitative weighting, which introduces context-dependency when applied across diverse industrial sectors. Wen-tao's (2012) case study on the Lifan Motorcycle Production Base also reported success in utilizing non-traditional water resources; adapting such high utilization rates (36%) to less resource-rich settings presents a valuable area for further research[26]. Boysen et al. (2020) provided a model-based economic and environmental assessment of water reuse, identifying economies of scale as a key factor[27], [28]. While highlighting the importance of scale, these findings also underscore the need to develop complementary, scalable frameworks that remain highly accessible to small and medium-sized enterprises (SMEs) within larger clusters [29].

2.1. Research gap and study objectives

While sophisticated spatial optimization models exist in broader resource management literature, they often rely on computationally intensive mathematical programming that assumes centralized control. A practical opportunity remains to unite water quality-based reuse optimization with spatially explicit pipeline routing using accessible, heuristic frameworks. For instance, foundational WPA techniques aim to minimize freshwater consumption and wastewater generation through systematic reuse strategies (such as in textile processing), and can be further enhanced by incorporating the spatial deployment of infrastructure [30]. Similarly, optimization models for eco-industrial parks often address transport network design and treatment technology choices, but do not jointly model reuse quality constraints and the resulting infrastructure trade-offs [31]. Furthermore, empirical studies calibrating this form of integrated, cost-aware modeling using real-world, brownfield industrial layouts and local regulatory standards remain limited. To bridge this methodological gap, this study develops and evaluates a specific hybrid framework integrating Water Pinch Analysis (WPA) and Geographic Information Systems (GIS), utilizing empirical data from 17 industrial facilities in the Port of Amsterdam. To strictly bound the scope of this evaluation, the specific objectives of this study are:

1 To identify feasible source-sink water reuse allocations based strictly on single-contaminant (chloride) compatibility, utilizing a rule-based Nearest Neighbor Algorithm (NNA) to execute the Water Pinch Analysis.
2 To incorporate physical infrastructure constraints into the network design by routing the WPA-generated connections through an established public road network using GIS spatial analysis and Dijkstra's shortest-path algorithm.
3 To evaluate the multi-objective trade-offs between maximizing freshwater savings and minimizing total pipeline length (serving as a surrogate for capital cost) by deriving a Pareto optimal front to support stakeholder decision-making.

3. Methodology

This study integrates well-established methods in water reuse optimization with Geographic Information Systems (GIS) to address both water quality and spatial infrastructure constraints in the industrial cluster at the Port of Amsterdam. The methodology builds on Water Pinch Analysis (WPA), originally developed by Wang and Smith (1994), and adapts it to the specific industrial and spatial dynamics of an industrial cluster [11]. Furthermore, a multi-objective optimization is integrated to understand the trade off and balance freshwater reduction goals with pipeline infrastructure, utilizing GIS for spatial planning and approximation.

3.1. Water allocation analysis

WPA is a widely recognized method for optimizing water use and reuse within industrial systems, minimizing freshwater consumption while recycling wastewater[28,29,32]. The approach systematically matches water sources, defined as wastewater streams from industrial processes, with water sinks, which are processes requiring water, based on contaminant concentrations. WPA was selected over alternative optimization-based approaches due to its transparency, interpretability, and minimal data requirements, making it particularly well-suited for early-stage planning across industrial clusters where detailed operational or economic data may be limited. Unlike mathematical programming methods (e.g., MILP, NLP), which often require exhaustive process-level parameters and assume centralized optimization control, WPA facilitates decentralized decision-making by visually identifying reuse opportunities based on water quality tiers. This makes it more accessible for multi-stakeholder environments with varied facility types and water demands. Furthermore, WPA's graphical foundation allows direct integration of quality thresholds, which aligns well with the regulatory focus of our case study (Port of Amsterdam). Importantly, WPA's qualitative clarity complements the spatial routing dimension added through GIS integration in our framework. Therefore, WPA was chosen not as a rejection of advanced mathematical programming methods, but as a strategic foundation for building a hybrid, spatially aware reuse planning tool.

In this application, WPA is applied to an eco-industrial park to identify opportunities for water reuse across 17 industrial facilities in the Port of Amsterdam. This algorithm was implemented in Python (v3.10) using the Pandas and NumPy libraries to enable efficient data handling, matrix operations, and iterative nearest-neighbor matching. The basic principles of WPA—matching available used water (‘sources’) and processes in demand of water (‘sinks’) based on contaminant concentrations—are well documented in the literature [13,16]. This study uses chloride as the primary contaminant, given its significant impact on both regulatory compliance and industrial performance related to the study location, which will be explained below, particularly in building material production and chemical processes. For instance, the NEN-EN 1008 (European standard for mixing water for concrete - Specification for sampling, testing and assessment of the suitability of water, including rinse water from cleaning installations in the concrete industry, as mixing water for concrete) has tabulated the maximum chloride content (450–4500 mg/l) of water for different end-use of the concrete. Furthermore, chloride is a conservative, non-reactive ion, which simplifies modeling its behavior across spatial reuse networks. The authors acknowledge that while chloride serves as a useful proxy for salinity and durability-related reuse applications (e.g., concrete production), the quantitative conclusions and Pareto front trade-offs generated in this study are strictly limited to single-contaminant matching scenarios. This approach does not reflect critical reuse constraints such as biodegradability, toxicity, or organic load, commonly represented by chemical oxygen demand (COD), biological oxygen demand (BOD), or heavy metals. These factors can also be particularly relevant in process water. However, based on stakeholder consultations during this study, multiple industries at the Port of Amsterdam indicated that chloride is their primary concern when considering reuse of neighboring industrial wastewater, since common contaminants like COD and BOD are already treated to standard discharge thresholds as mandated by the local water authority. The authors emphasize that the freshwater savings calculated herein represent a theoretical maximum or 'best-case' reuse potential under specific regulatory boundaries. In reality, the introduction of multi-contaminant constraints would inherently reduce the number of feasible source-sink matches, thereby lowering the total reuse volume and shifting the Pareto optimal front. Incorporating these multi-contaminant quality indices remains a necessary progression for generalizing this framework to broader industrial operations an important direction for future research as data availability improves.

Once source and sink data were collected, composite curves were constructed to identify the pinch point, following the method outlined by Sorin & Bédard (1999) [33]. The Source Composite Curve, which plots cumulative flow rates of wastewater sources in ascending order of the average contaminant concentration, was superimposed on the Sink Composite Curve, which arranges water-consuming processes by their allowable contaminant concentrations. The pinch point represents the minimum freshwater requirement necessary to meet the demands of all sinks while maximizing water reuse within the system. Thereafter, to facilitate source-sink allocation, a Nearest Neighbor Algorithm (NNA) was employed. This algorithm, following the approach described by Prakash & Shenoy (2005), systematically matches each sink with the nearest available source based on contaminant concentration, ensuring that water quality requirements are met without exceeding regulatory contaminant limits [34]. When the available non-freshwater sources could not fully satisfy the water demand of a sink, freshwater was allocated as a last resort. In this study, the algorithm is executed iteratively, incorporating a constraint to exclude the previously identified 'best' solution to explore alternative water exchange scenarios. To improve transparency, it is important to clarify that the NNA used in this study resets its allocation matrix at the beginning of each iteration. This means that each iteration starts with a fresh allocation based on updated constraints, such as excluding previously assigned source-sink pairs. This approach allows the algorithm to explore alternative configurations, avoiding local optima and enabling a broader exploration of the solution space. While the core matching logic remains consistent (selecting sources closest in contaminant concentration to each sink’s threshold), the source pool dynamically updates in each iteration to reflect prior exclusions. To ensure generalizability across any industrial cluster, the NNA incorporates two distinct, dynamically evaluated stopping criteria. First, the local allocation stopping criterion dictates that for any single network scenario, source-to-sink matching terminates only when the residual volumetric demand of all sinks is mathematically satisfied (target residual $<10^{-6}$ m^3/h), or when the inventory of feasible reuse sources is exhausted, prompting the algorithm to supply the remaining deficit with freshwater. The completeness guarantee rests on two properties of the exclusion strategy. First, at each iteration the highest-volume source-sink pair is banned, which is the pair that most strongly defines the current network topology. Removing it forces the algorithm into a structurally distinct configuration rather than a minor reallocation. Second, because each source has finite capacity and each sink has a fixed demand, the number of feasible non-freshwater pairings is bounded. Progressive exclusion therefore forms a finite, non-repeating sequence that must terminate at the all-freshwater baseline. In a cluster of n source-sink pairs, the maximum number of iterations before exhaustion is bounded by the number of unique feasible pairings, which for the 17-facility Port of Amsterdam dataset is 12. For larger clusters, this bound grows combinatorially, and the deterministic exhaustive approach used here would need to be replaced by a heuristic search such as genetic algorithms or simulated annealing to remain computationally tractable. To aid comprehension, a simplified pseudo-code of the iterative NNA is included below with the full results across iterations are presented in Table i in the Appendix:

```
For iteration in 1 to max_iterations:
  Reset all allocations
  For each sink:
  Identify all feasible sources (not previously used)
  Select nearest neighbor based on contaminant concentration
  Assign flow if capacity and quality constraints are met
  End For
  Record total freshwater use
  Update exclusion list for next iteration
  End For
```

To facilitate replication, the complete operational procedure of the

NNA is described below in pseudo-code. This directly reflects the implemented algorithm: sinks are processed strictest-first, sources are selected dirtiest-usable-first, and freshwater is introduced only when no reuse source can satisfy the remaining demand. The allocation resets fully at the start of each iteration, with previously used source-sink pairs progressively excluded to force exploration of alternative network configurations.

```
INPUT:
Sources: list of {name, available_volume (m³/h), contaminant_load (kg/h)}
Sinks: list of {name, required_volume (m³/h), max_allowable_load (kg/h)}
Exclusions: set of (source_name, sink_name) pairs banned in this iteration
INITIALISE:
total_freshwater ← 0
total_pipeline_distance ← 0
allocation_matrix ← empty
STEP 1 — Sort sinks in ascending order of max_allowable_load
// Strictest quality constraint served first; preserves
// cleanest sources for most constrained sinks
FOR EACH sink in sorted_sinks:
remaining_demand ← sink.required_volume
WHILE remaining_demand > convergence_tolerance:
STEP 2 — Identify feasible sources:
feasible ← all sources where:
(a) source.contaminant_load / source.available_volume
≤ sink.max_allowable_load / sink.required_volume
// Quality constraint: source concentration must not
// exceed sink's allowable concentration
(b) source.available_volume > minimum_flow_tolerance
// Capacity constraint: source must have volume remaining
(c) (source.name, sink.name) NOT IN exclusions
// Exclusion constraint: pair not banned this iteration
IF feasible is not empty:
STEP 3 — Select source:
selected ← source in feasible with HIGHEST contaminant concentration
// Dirtiest-usable-first: reserves cleaner sources
// for more constrained downstream sinks
STEP 4 — Allocate volume (mass balance):
allocated_volume ← MIN(selected.available_volume, remaining_demand)
selected.available_volume ← selected.available_volume - allocated_volume
remaining_demand ← remaining_demand - allocated_volume
STEP 5 — Record connection:
Add (selected.name → sink.name, allocated_volume) to allocation_matrix
Look up GIS Dijkstra distance for this source-sink pair
total_pipeline_distance ← total_pipeline_distance + GIS_distance
ELSE:
// No feasible reuse source available — default to freshwater
total_freshwater ← total_freshwater + remaining_demand
remaining_demand ← 0
END WHILE
END FOR
OUTPUT per iteration:
total_freshwater (m³/h)
total_pipeline_distance (km)
allocation_matrix
```

Every allocation satisfies three physical constraints by construction: (i) each sink receives exactly its required volume, supplemented by freshwater only if reuse sources are insufficient; (ii) no source supplies more than its available volume; and (iii) the contaminant concentration of allocated water never exceeds the sink's maximum allowable threshold. These constraints are enforced through the feasibility filter in Step 2 and the mass balance in Step 4 at every allocation step, without reliance on an external optimization solver.

3.2. Geographic information systems (GIS) integration

The spatial constraints of industrial clusters necessitate the integration of Geographic Information Systems (GIS) into water reuse planning and optimization. GIS provides a spatial analysis framework that addresses pipeline routing challenges, which are often overlooked in traditional WPA applications [35,36]. In this study, GIS was used to map the physical layout of an industrial cluster, as well as existing road networks. Given that the Port of Amsterdam is a highly developed industrial cluster within a metropolitan region, the routing methodology explicitly utilized the actual public road network (via OpenStreetMap) to define feasible corridors. This approach ensures that proposed pipelines realistically follow permissible infrastructure paths, inherently avoiding physical barriers, such as waterways, protected zones, and established private property, that would prevent direct routing. The adoption of GIS for pipeline routing is crucial when navigating spatial complexities that basic distance measures (like Euclidean or Manhattan distances) simply cannot capture. By constraining routes to the existing road network, the model reflects the practical reality of brownfield projects, where new infrastructure must align with established rights-of-way. The spatial constraints of industrial clusters necessitate the integration of Geographic Information Systems (GIS) into water reuse planning. GIS routing models help minimize the economic, environmental, and temporal costs of pipeline construction by effectively managing diverse datasets such as topography, land use, and regulatory exclusions [37]. In contrast, simple distance matrices can grossly underestimate actual pipeline lengths or recommend technically untenable paths.

By incorporating cost surfaces, least-cost path analysis, and multi-criteria decision-making, GIS reflects real-world constraints and enhances engineering accuracy and permit compliance, ultimately producing more actionable and stakeholder-relevant pipeline designs [38,39]. In the highly developed, brownfield context of the Port of Amsterdam, these real-world constraints manifest as impassable physical barriers, such as waterways, protected ecological zones, established building footprints, and private property boundaries. To explicitly incorporate these absolute barriers into our least-cost path analysis, all pipeline trajectories were strictly restricted to the established public road network, which represents the only legally and physically feasible corridor for new subsurface infrastructure. The spatial routing was executed using QGIS (v3.28) equipped with the built-in Network Analysis plugin. An OpenStreetMap-derived vector shapefile of the industrial road network was utilized to define the infrastructural boundary. The Dijkstra algorithm was then applied within this module to calculate the shortest permissible path along this constrained vector graph for every WPA-identified source-sink pair[40]. The critical linkage between the WPA outputs and the GIS spatial environment was established through geographic coordinate matching. The allocation matrix generated by the WPA algorithm, detailing the exact volumetric flow (m^3/h) assigned between specific source and sink IDs was exported and joined to a geospatial point layer representing the physical centroid of each industrial facility. By overlaying these WPA-generated pairings onto the spatial data, every theoretical water match was translated into a

definitive origin-destination (O-D) pair. Pipeline routing was then synthesized for each O-D pair using the Dijkstra Algorithm, which calculates the shortest path between these facility nodes exclusively along the constrained vector graph of the existing road network. By tying the pipeline lengths exclusively to these navigable corridors, the methodology successfully navigates real-world physical limitations, ultimately producing actionable and permitting-compliant pipeline designs.

3.3. Multi-objective optimization

To balance the competing objectives of minimizing freshwater consumption and minimizing total pipeline length (serving as a surrogate for infrastructure capital costs), multi-objective optimization was employed. Throughout this study, total pipeline length (km) serves as a spatial proxy for infrastructure capital burden. It captures the physical extent of required pipeline construction but does not assume direct cost equivalence; where cost figures are cited, they are explicitly attributed to published benchmarks and clearly distinguished from the spatial metric. A Pareto Front Analysis was conducted to evaluate the trade-offs between reducing freshwater use and minimizing the total pipeline length required to transport water between facilities [41]. The Pareto Front represents a set of optimal solutions, each of which balances environmental sustainability and economic considerations. This analysis provided decision-makers with insight into the trade-offs involved in maximizing freshwater savings while minimizing total pipeline length, that can serves as the direct physical proxy for capital infrastructure cost.

This outcome was enabled by a sequential integration of the WPA and GIS modules. Initially, feasible source–sink reuse pairs were identified based on chloride concentration thresholds using WPA. For each unique solution generated (e.g., Iteration 0, 1, etc.), the specific set of identified matches was translated into a network topology. Every matched source-sink pair was treated as a required physical connection, which was then individually routed through permissible infrastructure corridors via the Dijkstra algorithm within QGIS (v3.28) using the Network Analysis plugin [42]. The resulting pipeline lengths were summed to calculate the total infrastructure footprint for that specific reuse scenario, used alongside the corresponding reused water volumes to populate a trade-off space.

To evaluate the multi-objective trade-offs between these two metrics, non-dominated sorting was applied to the full set of network configurations generated across NNA iterations. Each configuration is evaluated against two minimization objectives: f_1 representing total freshwater demand (m^3/h) and f_2 representing aggregate GIS-routed pipeline length (km). A solution i is defined to strictly dominate solution j if and only if $f_1(i) \leq f_1(j)$ and $f_2(i) \leq f_2(j)$, with at least one strict inequality holding. The Pareto-optimal front is the subset of configurations for which no such dominating solution exists. This sorting was implemented in Python using a pairwise Boolean comparison matrix via NumPy, as detailed in the pseudo-code below.

```
PARETO OUTER LOOP (Pareto space generation)
INPUT:
Sources, Sinks (same as NNA Inner Loop)
INITIALISE:
exclusions ← empty set
solutions ← empty list
FOR iteration = 0, 1, 2, ...:
STEP 1 — Reset source volumes to original values
STEP 2 — Run NNA Inner Loop with current exclusions
→ returns (total_freshwater, total_pipeline_dis
tance,
allocation_matrix)
STEP 3 — Record solution:
Add (total_freshwater, total_pipeline_distance)
to solutions
STEP 4 — Check stopping criterion:
IF allocation_matrix contains no reuse pairs
(100% freshwater, baseline reached):
STOP
// All viable source-sink combinations exhausted;
// complete trade-off space has been explored
STEP 5 — Update exclusions:
Identify highest-volume pair in allocation_matrix
Add (source.name, sink.name) to exclusions
// Banning the dominant match forces a structurally
// different network topology next iteration
END FOR
STEP 6 — Extract Pareto-optimal front:
FOR EACH solution i in solutions:
dominated ← FALSE
FOR EACH solution j in solutions (j ≠ i):
IF j.freshwater ≤ i.freshwater AND
j.distance ≤ i.distance AND
at least one strict inequality:
dominated ← TRUE; BREAK
IF NOT dominated:
Add solution i to Pareto front
OUTPUT:
Pareto-optimal front: set of non-dominated
(freshwater, pipeline_distance)
```

This structured workflow ensured that both water quality combability and spatial feasibility were incorporated, allowing decision-makers to explore operational strategies that reflect the spatial realities of industrial reuse implementation. In the present case study this outer loop converged after 12 iterations, at which point progressive exclusions depleted all viable reuse combinations and the system returned to its 79.2 m^3/h baseline, confirming complete exploration of the trade-off space. The detailed results across all iterations are tabulated in Table i in the Appendix.

3.4. Case study description and data collection

This paper uses a case study to examine the above methodology in supporting the circular water initiative of an industrial cluster. The Port of Amsterdam, a key global maritime hub, has become a leader in integrating circular economy principles into its industrial and water management practices. Concrete examples include the Port of Amsterdam Circular Hub, which recycles and repurposes materials like plastics, metals, and organic waste, attracting companies that turn waste into new products, thus reducing landfill use and conserving resources. These initiatives mitigate environmental impacts and improve resource efficiency [43].

In the Amsterdam metropolitan area, climate change, population growth, and urbanization are reducing freshwater availability while increasing demand, leading to potential water shortages within 10 years. Research into alternative water sources is necessary to ensure future supply [44]. This study focuses on industries connected to the Westport Area's industrial water network, established in the 1960s. The network supplies approximately 1.75 million m^3 of pre-treated water annually to 17 companies, including producers of concrete products, a waste-to-energy facility, biofuel manufacturers, and chemical plants. The selection of 17 industries was based on availability of reliable water usage and discharge data from the local utilities and environmental agency in Amsterdam and the spatial proximity within the boundary of Port of Amsterdam. Industries without publicly reported or shared water data, or those located outside the port area, were excluded from analysis. While this may introduce a selection bias, the impact on the purpose of the study is considered minimal. Under the European Pollutant Release and Transfer Register (E-PRTR) Regulation (EC) No 166/2006 and the Dutch Electronic Annual Environmental Report (e-MJV) framework, public reporting is mandatory only for facilities exceeding specific capacity thresholds or pollutant discharge limits. Consequently,

facilities absent from these public datasets are assumed to play a relatively small role in receiving and providing water within the context of this study [51]. While the exclusion of non-reporting facilities introduces a selection bias, its analytical impact directly shapes the techno-economic feasibility of the model. Because the regulatory thresholds filter out micro-consumers, the resulting dataset systematically isolates the high-volume actors responsible for the vast majority of the cluster's water footprint. Consequently, the proposed reuse network represents a refined, high-yield 'macro-backbone' of the port. From a spatial optimization perspective, integrating the excluded, sub-threshold facilities would introduce disproportionately high spatial complexity and pipeline infrastructure costs for statistically marginal volumetric water savings. Therefore, this system boundary accurately captures the most viable tier for industrial symbiosis, ensuring that the dataset reflects realistic, high-impact spatial linkages and heterogeneous reuse potentials within the modeled cluster.

The municipality of Amsterdam aims to reduce drinking water use for industrial purposes. On 31 May 2022, they adopted the Industrial Water Task, commissioning Waternet (the local water utility) to expand the industrial water network, which will double supply within 5 years due to growing needs from existing and new water-intensive industries such as data centers and hydrogen production facilities [45],. The security of water supply to these industries may be further impacted by the implementation of a precedence list for water allocation during scarcity and the National Plan for Drinking Water Conservation. The precedence list significantly impacts industries. While it ensures the continuity of essential services by prioritizing critical sectors such as food production, healthcare, and heat and power generation, it can also disrupt operations in less critical industries. The potential for fluctuations in the priority list based on changing water availability introduces an element of uncertainty for all industries. To mitigate these challenges, businesses should prioritize water efficiency, explore alternative water supply options, and develop robust contingency plans. The revised Urban Wastewater Treatment Directive has been promoting the reuse of treated wastewater to support the EU's circular economy objectives. Additionally, the local National Plan for Drinking Water Conservation complements this effort by aiming to reduce drinking water consumption through public awareness campaigns, regulations, and incentives [47]. This profoundly impacts industries, demanding substantial shifts in operational practices such as the shift from drinking water to a more fit for purpose industrial grade water. While these measures incur initial costs, they foster innovation, leading to long-term operational efficiency gains and reduced vulnerability to water scarcity.

A study from van der Hoek et al., (2016) presented that Amsterdam's wastewater offers a huge potential for resource recovery. However, it is hampered by a lack of planning and design methodology [48]. Furthermore, reuse of water was not considered in that study, but as the security of water supply (for industry) is becoming an increasing concern, presenting a gap for further research. Valentine (2016) identifies four key factors for successful collaboration: a shared environmental focus, opportunities for joint projects, mutual benefits, and shared challenges requiring collective solutions. The authors argue there is an additional key factor that should be explicitly acknowledged is the role of supporting policies and governance. In the case of Amsterdam, organizations such as the municipality, water utilities and the local environmental agency play a crucial role in driving collaborative efforts by actively shaping governance frameworks and policies that enable sustainable water management. The Port of Amsterdam offers a prime example of an environment where these factors converge, making it an ideal setting to study collaborative innovation for sustainable water management [49].

Data for this study, which focuses on the input and output of water and pollutant load in industrial facilities, were collected from multiple sources, including industrial water customers, local water utilities (both drinking and wastewater: Waternet and Waterschap Amstel, Gooi en Vecht, respectively), local environmental agencies (Omgevingsdienst Noordzeekanaalgebied), and the European Pollutant Transfer Register (EPTR). This study assumes a progressively reducing water quality for different processes based on the maximum allowable contractual concentration, aligning with the heuristic rules of water pinch analysis to identify optimal water reuse opportunities [50]. Water usage data were obtained as annual totals (m^3/year) for each industry based on the recent reporting year with the complete dataset (2023). To standardize inputs for the WPA model, these values were converted into average hourly flow rates using the following assumption: industries operate approximately 365 days per year and run a continuous 24 h operational shift per day. The conversion formula used was:

$$\text{Hourly Flow Rate } (m^3/\text{h}) = \text{Annual Water Use } (m^3/\text{year}) \div 365 \text{ days} \div 24 \text{ h}.$$

This simplification enables consistent comparison across industries with varying scales. While this simplification enables consistent comparison across industries with varying scales, it constitutes a fundamental limitation that significantly impacts the operational reliability of the model. By assuming continuous operation, the analysis effectively 'smoothens' the temporal peaks and troughs inherent in batch processing, maintenance shutdowns, and seasonal variations. Consequently, the derived pinch analysis assumes perfect temporal alignment between source availability and sink demand. In reality, industrial operations are often asynchronous. For example, a batch-process source might release wastewater when a potential sink is offline or at low demand. To capture this theoretical reuse potential in a real-world setting, buffer tanks would be required to store volumes during supply peaks for use during demand peaks. Therefore, the results presented here should be interpreted as the theoretical steady-state reuse potential, acting as an upper bound compared to the operational reliability achievable without intermediate buffering. Consequently, the steady-state freshwater savings calculated here are highly likely to overestimate the realistically achievable reuse volumes. Quantifying these necessary buffer capacities through dynamic modeling represents a potential future research to translate these theoretical targets into actionable infrastructure designs. The hourly flow requirement of industrial water demand was estimated based on the yearly contractual water use of these industries, while the potential supply or source was estimated from the yearly discharge records of the companies, obtained from the local environmental agency [51].

Additionally, the model currently relies on cross-sectional data from the 2023 operational year. While this provides a recent and stable baseline, it represents a static temporal snapshot that inherently fails to capture long-term industrial life cycles, economic downturns, or phased facility expansions. Consequently, a formal statistical uncertainty propagation was omitted due to the absence of empirical variance distributions for this single-year baseline, meaning the derived Pareto front solutions represent a deterministic steady-state boundary rather than a probabilistic range. Relying on a single-year water balance to dictate the spatial layout of rigid, capital-intensive pipeline infrastructure introduces a significant risk of 'infrastructure lock-in.' For instance, if a primary source industry ceases operations or alters its process chemistry over the next decade, the associated downstream pipelines may become stranded assets, rendering the calculated Pareto configurations obsolete. Conversely, unpredicted expansions could result in severely undersized hydraulic capacities. Therefore, from a long-term municipal planning perspective, the network topologies proposed herein must be viewed as an initial baseline rather than a final schematic. Future planning phases must integrate multi-year longitudinal datasets and stochastic demand forecasting to ensure the proposed infrastructure possesses the modularity and hydraulic flexibility required to withstand inter-annual volatility.

Furthermore, this study concentrates exclusively on the users of industrial grade water within the supply system of the scope to be the 'demand' for the water pinch analysis, excluding the supply of drinking

water to industries due to data privacy concerns. While this exclusion limits the ability to create a fully comprehensive water profile for the study area, the methodology remains valid. Industrial-grade water, being of lower quality than drinking water, is typically used in processes with higher tolerance for water quality variations, making it well-suited for a fit-for-purpose and circular water management approach. Large drinking water consumers, such as industries, could be potential sources of alternative water. However, in many cases, water is either absorbed into products or becomes too contaminated for direct reuse, as seen in the case study. Reusing wastewater that originates from drinking water is a preferable option in this context, as it generally maintains higher quality, making treatment and reuse in industrial processes more feasible. This approach further reinforces circular water management practices.

4. Results and discussion

The study presents the application of WPA in combination with GIS providing a hybrid framework to assess and optimize water reuse potential within the industrial cluster at the Port of Amsterdam. This section presents the key findings from the analysis, focusing on the identification of opportunities for optimizing water use and addressing constraints related to water quality and infrastructure. These results are discussed in relation to the three main research objectives: (1) identifying feasible reuse pairs based on water quality compatibility, (2) incorporating spatial constraints into network design, and (3) evaluating trade-offs between water savings and infrastructure requirements. Among the industries consulted and analyzed, the building materials sector emerged as the median in terms of the type of industry, making it a representative benchmark for assessing chloride contamination's impact on reuse strategies. Chloride ingress into concrete from contaminated water sources, can lead to severe deterioration of concrete structures. This is due to mechanisms such as chloride-induced corrosion of steel reinforcement and the formation of expansive compounds that compromise structural integrity [34,35]. Therefore, addressing chloride contamination as the key contaminant for this study is essential for ensuring the viability and sustainability of water reuse practices. However, in practice, this approach may not fully represent reuse feasibility for industries concerned with other contaminants such as BOD or heavy metals. Incorporating additional contaminants to the current method could be an important direction for future research.

The results of the WPA and NNA applied to the industrial cluster at the Port of Amsterdam provide a comprehensive understanding of the water reuse potential within the system. The overview of the inventory of sources (available used water) and sinks (water demands), as well as the results from the first iteration of nearest neighbour algorithm is presented in Table 1.

A composite curve is then plotted in Fig. 1, representing the water quality plotted against cumulative water flow rates of the system to visually identify the pinch point and determine the minimum freshwater requirement for the process. The curve reveals that the system has a minimum freshwater requirement of 10.3 m^3/h. This minimum threshold represents the baseline freshwater demand needed to manage the pollutant load, even with optimized water reuse. The graph highlights a pinch point, where the sink flow (water demand) and source flow (water supply) intersect, a critical threshold for system optimization. This point marks the system's limitation in further reducing freshwater consumption, as any attempts to cut water use beyond this

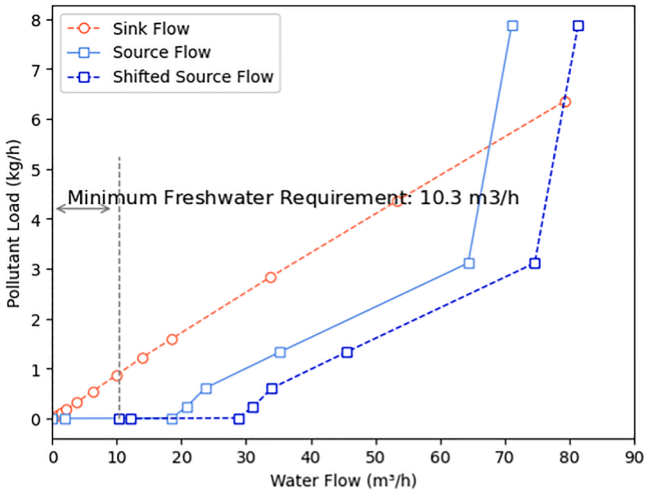


Fig. 1. The composite curves for determining pinch points in terms of chloride as key contaminant.

Table 1
Characteristics of the quantity and quality of allocated water reuse using chloride as key contaminant, resulted from the first iteration of nearest neighbour algorithm.

Sink	Source	Allocated Water (m^3/h)[a]	Allocated Concentration (mg/l)[b]	Source Load (kg/h)	Sink max Load (kg/h)	Sink Max Concentration (mg/l)[c]
Cleaning 1	Freshwater	0.46	0.00	0.00	0.038	83
Building Material 5	Freshwater	0.46	0.00	0.00	0.039	86
Building Material 4	Freshwater	0.57	0.00	0.00	0.056	87
Metal coating 1	Freshwater	0.68	0.00	0.00	0.06	80
Building Material 6	Freshwater	1.60	0.00	0.00	0.14	85
Building Material 1	Freshwater	2.51	0.00	0.00	0.22	90
Building Material 3	Freshwater	3.65	0.00	0.00	0.32	88
Building Material 2	Freshwater	0.44	0.18	0.00	0.36	89
Building Material 2	Chemical A	1.89	0.18	0.00022	0.36	89
Building Material 2	Food A	1.66	0.18	0.00051	0.36	89
Chemical 1	Food A	4.57	0.11	0.00051	0.37	82
Chemical 2	Food A	10.4	4.06	0.00051	1.2	81
Chemical 2	Food B	4.82	4.06	0.061	1.2	81
Energy 1	Food B	20	3.1	0.061	1.5	78
Building Material 7	Food B	4.7	41	0.061	2.0	77
Building Material 7	Energy A	11	41	0.063	2.0	77
Building Material 7	Biofuel A	2.27	41	0.096	2.0	77

[a] "Allocated Water" refers to the volume of water assigned to a specific industrial process based on water reuse optimization, ensuring that water quality constraints are met while minimizing freshwater consumption. Estimated based on annual contractual value.

[b] "Allocated Concentration" denotes the contaminant concentration in the allocated water, reflecting the quality of the reused water supplied to each process, as determined by the nearest neighbor algorithm.".

[c] Progressively reducing water quality for different industries based on the maximum contractual allowable concentration, aligning with the heuristic rules of water pinch analysis to identify optimal water reuse opportunities.

point would exceed the system's capacity to handle the pollutant load. Thus, the pinch point defines the maximum level of water optimization that can be achieved under the current system configuration without additional treatment or infrastructure, which aligns with the study by Sorin & Bédard (1999). It discusses the infeasibility of water reuse strategies above the pinch point due to the constraints on contaminant concentrations and the effectiveness of water reuse below the pinch point [33]. This is a key concept in understanding why water reuse above the pinch point is often not feasible. While these results demonstrate successful freshwater reduction, it must be emphasized that these refined allocations and the resulting 10.3 m^3/h target are strictly valid only for single-contaminant (chloride) matching scenarios. This choice was intentional based on regulatory relevance and data consistency. While this is an important contaminant in the context of concrete production. In reality, industries deal with complex, multi-contaminant wastewater (e.g., BOD, heavy metals). Evaluating these overlapping discharge profiles would inherently restrict feasible matches and alter the ultimate reuse potential [52]. In addressing the first research question, these results confirm that chloride-based WPA is effective for identifying feasible reuse paths, particularly in sectors like building materials where chloride poses a durability risk. However, this approach may not fully represent reuse feasibility for industries concerned with other contaminants such as BOD or heavy metals. In addition to the chemical-specific limitations discussed, the model's reliance on converting annual data into 24/7 constant hourly flows severely limits the practical reliability of the proposed network. Because industrial operations are highly asynchronous driven by shift work, batch production, and maintenance, this steady-state assumption inherently masks the temporal mismatch between wastewater generation and process demand. As a result, the infrastructure footprints and water savings calculated in these Pareto solutions are theoretically optimal but operationally vulnerable, as they do not account for the storage infrastructure required to buffer these peak loads. Such non-synchronous start/finish times reduce direct reuse opportunities; intentional waiting or rescheduling can increase reuse by aligning sources and sinks in time [53,54]. To incorporate such variability, future iterations of this framework could adopt scenario-based models or dynamic programming methods. These approaches divide the planning horizon into time blocks (e.g., hourly or daily) and optimize water reuse allocations under shifting supply-demand conditions. Similar methods have been used in prior studies, under different scenario assumptions on decentralized urban reuse planning and large transfer projects [55–57]. Their integration into WPA-GIS frameworks would enhance realism and decision-making relevance for reuse planning under operational uncertainty in future studies.

In relation to the third research objective of evaluating trade-offs between reuse potential and infrastructure, Figs. 2 through 5 demonstrate how reuse volumes and pipeline distances evolve across different optimization scenarios. Fig. 2 shows the allocated flows from sources to sinks from the results of the algorithm. For lower water demand industries, such as Cleaning 1, Building Material 5, and Building Material 4, the algorithm allocated freshwater due to the strict contaminant load limits of 0.038 kg/h, 0.039 kg/h and 0.050 kg/h, respectively. These sinks required 0.46 to 0.57 m^3/h of freshwater each to maintain operational efficiency. As the tolerance for contaminant loads increased, the allocation shifted to non-freshwater sources. For example, Building Material 2 was supplied with 1.89 m^3/h from Chemical A and 1.66 m^3/h from Food A, with contaminant loads of 2.2×10^{-4} kg/h and 5.1×10^{-4} kg/h, respectively, both well within the maximum allowable load of 0.36 kg/h for this process. Similarly, Chemical 1 and Chemical 2 received water from Food A and Food B sources, with maximum allowable loads of 0.37 kg/h and 1.2 kg/h, respectively.

The most water-intensive sink, Energy 1, required approximately 20 m^3/h of water from Food B, with a contaminant load of 0.061 kg/h, significantly below its maximum permissible load of 1.53 kg/h. For Building Material 7, which had the highest tolerance for contaminants (up to 2.00 kg/h), the algorithm allocated water from multiple non-freshwater sources, including Food B, Energy A, and Biofuel A. The results from this allocation demonstrate that the algorithm effectively minimized the use of freshwater by prioritizing wastewater reuse where contaminant levels were within acceptable ranges. The allocation logic ensured that only processes with very low contaminant tolerance were supplied with freshwater, while higher tolerance processes made use of treated wastewater, thus reducing the overall dependency on freshwater resources. These findings underscore the potential of source-sink matching using contaminant thresholds to prioritize industrial reuse without universal infrastructure upgrades. However, integrating multiple contaminants in future iterations may challenge these allocations, especially for sectors with overlapping discharge profiles.

Applying the global iterative stopping criterion, the algorithm systematically generated alternative network configurations by excluding prior 'best' matches. This exploration naturally terminated after

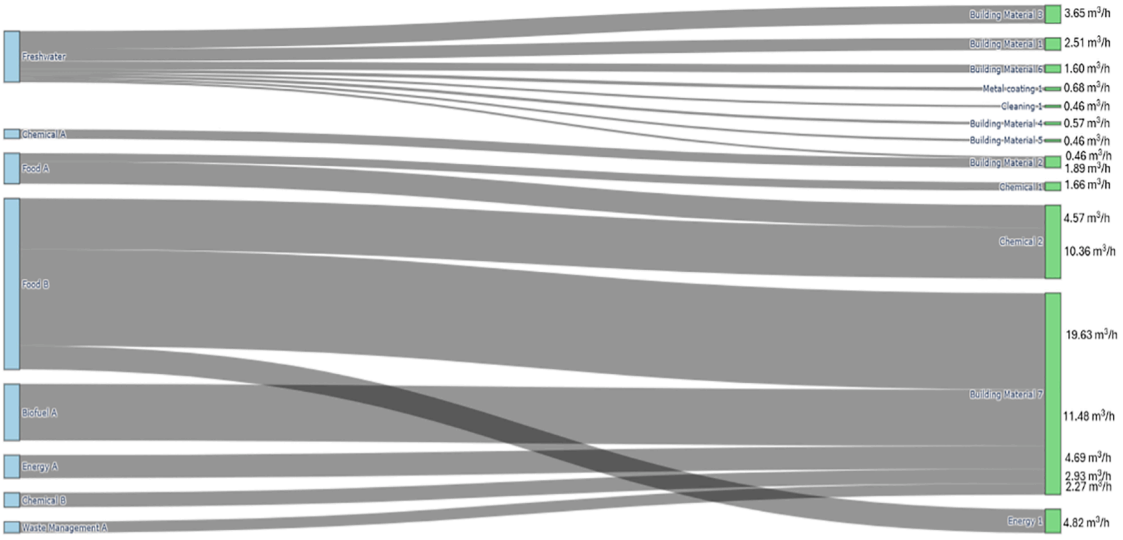


Fig. 2. Minimum freshwater network allocation by nearest neighbor algorithm. The arrows illustrate the connections between water sources (blue-labeled) and sinks (green-labeled) with edges representing water flow. The thickness of each edge is proportional to the allocated water (in m^3/h). Sources are effectively matched to sinks based on water quality criteria, minimizing freshwater consumption and wastewater generation.

generating 12 unique scenarios, at which point the progressive exclusion constraints depleted the pool of viable reuse matches, forcing the system to return to its 79.2 m^3/h baseline. This confirms the complete exploration of the Pareto space for this specific cluster. The detailed results across all iterations are tabulated in Table i in the Appendix. Each iteration depicts a different water exchange matrix, similar to Fig. 2. The number of unsatisfied sinks remained zero throughout all iterations, indicating that the algorithm successfully allocated water to all sinks without exceeding their maximum contaminant limits or flow capacity, due to the assumption of an unlimited freshwater supply to supplement. These iterative improvements simulate real-world decision-making, where reuse networks evolve through successive agreements or infrastructure expansions, making the algorithm practical for phased implementation. However, as the iterations progressed, the algorithm reached a point where further optimization using non-freshwater sources was not feasible, and the reliance on freshwater sources increased. The total freshwater required in each iteration varied as the algorithm refined its allocations. In the initial iteration (Iteration 0), the total freshwater requirement was 10.3 m^3/h (minimum freshwater required determined by Water Pinch Analysis). This increased as the algorithm reallocated sources and explored different combinations. After subsequent iterations, the algorithm refined the allocation to a point where only freshwater was used in Iteration 11, resulting in a final freshwater demand of 79.2 m^3/h (as is).

The second objective of this paper is to integrate spatial constraints (pipeline distance, infrastructure feasibility) via GIS-based routing to the scenarios developed above. The results from the shortest paths calculated using the Dijkstra algorithm with road data, reveal several key statistics that offer insights into the efficiency and variability of the water distribution network. The summary of all the results is demonstrated in Fig. 3. The mean distance, or average path length, is approximately 1.98 km, indicating a relatively short and efficient routing overall between the industries within the study scope. To contextualize this, the studied industrial cluster covers a total footprint of approximately 12 km^2 [43]. The fact that average connection lengths span only a fraction of the cluster's extent indicates a high degree of spatial proximity, driven by the historical zoning of heavy industries. Economically, these short transmission distances are significant: they imply reduced capital expenditures (CAPEX) for piping and lower hydraulic head losses (OPEX) compared to more dispersed industrial regions. This confirms that the port's physical layout is inherently conducive to decentralized water exchange. The median distance is slightly lower at 1.77 km, suggesting that the majority of the routes are even shorter, with half of the distances falling below this value. The standard deviation of 1.1 km indicates some differences in path lengths but not extreme outliers. The shortest recorded distance is nearly negligible at 5 m, while the maximum distance stretches to 5 km, indicating the presence of more distant connections within the network. This distribution suggests that many potential water reuse connections can be made over relatively short distances, which would minimize the need for extensive pipeline infrastructure. Such short distances present a cost-effective opportunity for pipeline routing, where shorter pipelines reduce both installation and maintenance costs. These statistics highlight the range and distribution of distances within the optimized water distribution network, providing a useful baseline for Pareto front optimization. To provide a direct performance benchmark of the integrated WPA–GIS framework against a conventional WPA-only approach, the source-sink pairs from Solution 0 were evaluated under two distance assumptions: Euclidean straight-line distances, representing the implicit spatial assumption of a standalone WPA application, and GIS road-network distances, representing the spatially constrained routing of the present framework. The mean Euclidean distance between matched pairs was approximately 1.3 km, compared to the mean road-network distance of 1.98 km. Across the full Solution 0 network, a WPA-only Euclidean estimate would project a total pipeline requirement of approximately 26 km, compared to the 39.4 km derived by GIS routing. This demonstrates a systematic underestimation of 34%, equivalent to 13.4 km of unaccounted infrastructure. This quantifies a concrete planning risk: a decision-maker relying on WPA alone would underbudget pipeline infrastructure by more than one-third, potentially rendering the chosen Pareto solution financially or technically infeasible during implementation. The GIS integration therefore adds demonstrable, quantified value beyond what the WPA component alone can provide, particularly in brownfield industrial contexts where physical barriers prevent direct routing.

The Pareto front was calculated to identify the optimal trade-offs between minimizing freshwater consumption and total pipeline length for water distribution. The solutions on the Pareto front represent those that strike the best balance between these two objectives, where improvements in one (e.g., reducing freshwater consumption) would result in compromises in the other (e.g., increasing transportation distance). The Pareto front analysis reveals key trade-offs between freshwater consumption and pipeline length in optimizing the water reuse network as demonstrated in Fig. 4. Solution 0, derived from the earlier WPA and NNA, required a pipeline length of 39.4 km and achieved a freshwater consumption of 10.3 m^3/h, representing an optimized solution based on chloride contaminant constraints. The results reasonably align with previous study on the UK's National Industrial Symbiosis Programme

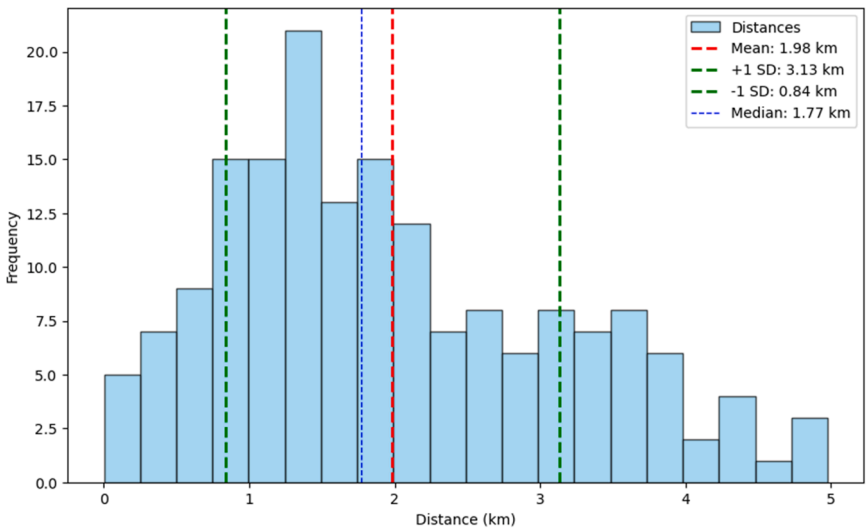


Fig. 3. The distribution of distances from the sources to the sinks within the scope of the study, along with the mean, standard deviation and median.

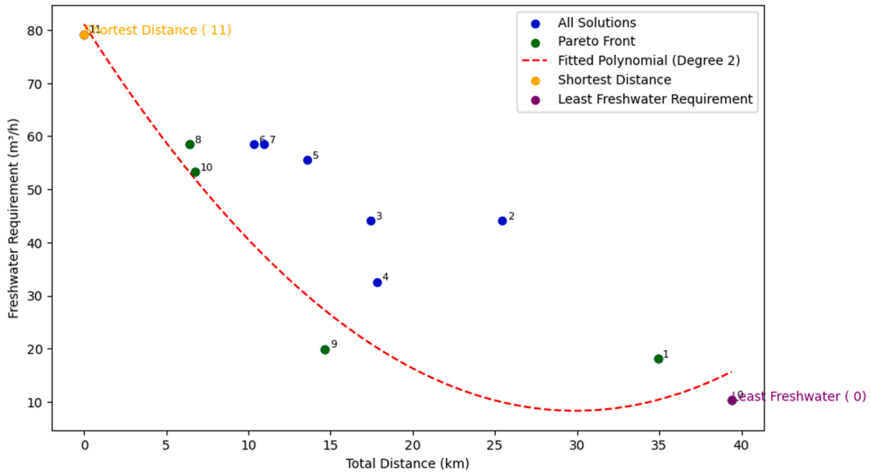


Fig. 4. Graph illustrating potential water management solutions, each solution depicts an iteration from Table with Pareto-optimal solutions highlighted representing the best trade-offs between minimizing freshwater consumption (y-axis) and distance (x-axis). The best-fit line shows the overall relationship between these two competing objectives.

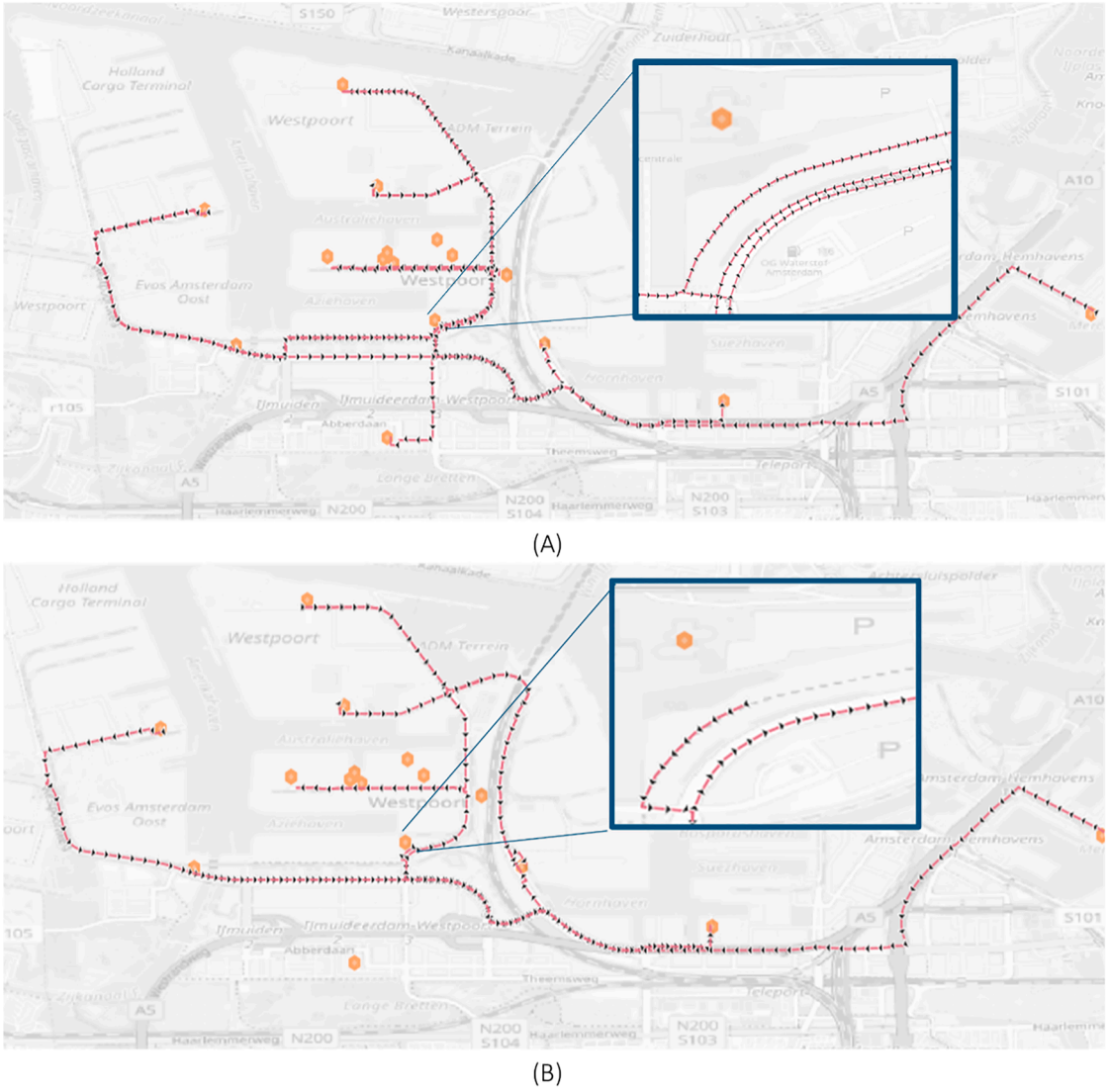


Fig. 5. Shortest water transportation infrastructure transportation pathway for solution 1 (A) and solution 9 (B). Both are on the Pareto Front with different trade off.

(NISP), as it found that the median distance materials travel between companies in symbiotic relationships is 32.8 km, based on an analysis of 792 synergies. This 32.8 km benchmark could serve as a useful indicator of geographic proximity in industrial symbiosis for similarly industrialized nations [46]. A structural analysis of the Solution 0 allocation matrix (Table 1) reveals that the reuse network is heavily concentrated around two source industries. Food B alone supplies 29.5 m^3/h across three sinks (Energy 1, Building Material 7, and Chemical 2), accounting for approximately 43% of the total non-freshwater allocation in the optimal scenario. Food A contributes a further 16.6 m^3/h across three sinks. Together, these two sources enable 67% of the total reuse volume in Solution 0. This concentration introduces structural vulnerability: if either facility reduces or ceases discharge, the Pareto-optimal network topology becomes infeasible, and the system would shift toward higher freshwater dependency. This finding underscores that the proposed network functions as a hub-and-spoke structure (centralized governance) rather than a distributed mesh, which has direct implications for long-term infrastructure resilience and the sequencing of bilateral reuse agreements.

As the network was further optimized, Solution 1 reduced the pipeline length requirement to 34.9 km, though freshwater requirement increased to 18.1 m^3/h, showing that reducing infrastructure can sometimes come at the cost of increased water usage. Solution 9 offered a trade-off, with a pipeline length of 14.7 km and a freshwater consumption of 19.9 m^3/h, providing an efficient compromise between minimizing infrastructure as depicted in Fig. 5 and achieving water savings.

In contrast, Solution 8 reduced the pipeline length to 6.4 km but required a higher freshwater consumption of 58.5 m^3/h, demonstrating the trade-offs involved in minimizing infrastructure investments. Solution 11 represents the “as-is” situation, where freshwater is the sole source and no additional infrastructure is required, resulting in a freshwater consumption of 79.2 m^3/h. This highlights the significant reliance on freshwater in the absence of an established reuse network. While this solution incurs no infrastructure costs, it is environmentally unsustainable due to the high freshwater consumption.

When comparing Pareto front solutions with non-Pareto solutions, the inefficiency of the latter became clear. For example, Solution 2, a non-Pareto solution, achieved a freshwater consumption of 44.1 m^3/h but required a pipeline length of 25.5 km, which is longer than the more efficient Solution 9 that achieved a much lower freshwater consumption of 19.9 m^3/h with a pipeline length of only 14.7 km. This demonstrated that non-Pareto solutions, despite requiring longer pipelines, do not deliver proportional water savings, making them less efficient from both an infrastructure and environmental standpoint.

From a decision-making perspective, the Pareto front can be operationalized through a structured three-tier framework that maps each solution to a distinct stakeholder profile, investment horizon, and risk tolerance, moving beyond descriptive observation toward actionable guidance.

Tier 1: Drought Resilience Priority (Solution 0: 39.4 km, 10.3 m^3/h freshwater).

This solution is appropriate for stakeholders whose primary driver is supply security rather than cost minimization. By reducing freshwater demand to the theoretical single-contaminant minimum, it provides maximum insulation against external supply interruptions during regulatory rationing events, effectively functioning as an infrastructure-based insurance policy. However, the illustrative annualized infrastructure cost of approximately €1.08 million (at ~€27,580/km/year) yields a break-even cost of ~€1.80/m^3 of saved water, which is only marginally above the current regional drinking water tariff of ~€1.76/m^3. Consequently, this tier is economically justifiable only when factoring in non-tariff risk costs such as business interruption, regulatory penalties, or anticipated tariff escalation under the revised Urban Wastewater Treatment Directive. Municipal authorities or large anchor industries with long planning horizons (>15 years) and formal water security obligations are the most natural adopters.

Tier 2: Cost-Optimized Compromise (Solution 9: 14.7 km, 19.9 m^3/h freshwater).

This solution represents the knee of the Pareto curve, where the point of maximum marginal return on infrastructure investment. It achieves approximately 75% of the theoretical maximum water saving while requiring <38% of the pipeline infrastructure of Solution 0. The illustrative annualized cost of ~€405,000 translates to roughly €0.78/m^3 of saved water, well below the current drinking water tariff, implying an immediate positive return on investment. This profile is most suitable for small-to-medium enterprises (SMEs) or industrial park operators seeking a near-term business case, where capital expenditure must be justified within standard payback periods of 5–10 years. It also represents a natural Phase 1 entry point for a phased implementation strategy, where infrastructure can later be extended toward Solution 0 as demand grows and financing conditions improve.

Tier 3: Business-as-Usual Baseline (Solution 11: 0 km, 79.2 m^3/h freshwater).

While requiring no capital investment, this scenario leaves the cluster fully exposed to rising freshwater tariffs and potential supply rationing. It serves as the quantitative reference point against which the value of all reuse investments must be calculated. Given Amsterdam's projected water scarcity within a 10-year horizon and the municipality's active expansion of industrial water pricing, continued reliance on this baseline represents a growing long-term financial and operational risk.

The Pareto front optimization results also revealed that significant reductions in freshwater usage can be achieved with relatively small increases in infrastructure investment, up to a point. Beyond that, the trade-offs become more pronounced, supporting Gunantara's (2018) findings that diminishing returns are an inherent feature of multi-objective optimization [41]. This understanding of the cost-benefit relationship in water reuse systems provides clarity on the economic feasibility of such systems, especially for small to medium-sized enterprises (SMEs). Prior research, such as Boysen et al. (2020), has noted that economies of scale tend to favor larger enterprises, but this study highlights specific points where collaborative models, forming a symbiotic supply chain or shared infrastructure could help smaller enterprises access the same sustainability benefits without prohibitive costs [27]. To transition these tiers from static observations into dynamic, long-term planning instruments, the topological trade-offs can be expressed mathematically. As demonstrated in Fig. 4, the Pareto front is not linear; it adheres to a second-degree polynomial regression. The first derivative of the fitted second-degree polynomial Pareto curve can be used to define a marginal cost threshold, the precise point on the curve where the incremental infrastructure cost per unit of freshwater saved exceeds the stakeholder's acceptable cost-benefit ratio. When pipeline length is used as a cost proxy, this derivative-based threshold allows planners to programmatically define a "cut-off coordinate" beyond which additional investment yields diminishing returns. For example, a municipality setting a maximum acceptable infrastructure cost of €1.00/m^3 of saved water would place its investment cut-off between Solutions 9 and 0, confirming that the 14.7 km network represents the rational upper bound under current tariff conditions.

It is important to note that this decision framework inherits the limitations of the underlying model. Because all Pareto solutions here are derived from single-contaminant (chloride) matching under steady-state assumptions, the freshwater savings cited in each tier represent theoretical upper bounds. In practice, introducing multi-contaminant constraints or temporal asynchrony between sources and sinks would shift the Pareto front inward, reducing feasible savings and potentially re-ranking the cost-effectiveness of individual solutions. Stakeholders should therefore treat these tiers as indicative planning benchmarks rather than operationally guaranteed outcomes, and validate selections against site-specific dynamic data before committing to capital investment.

While pipeline length serves as a spatial proxy for infrastructure

burden in this study, translating these distances into practical cost terms is essential for grounding the Pareto front in stakeholder decision-making. The European Benchmarking Co-operation (EBC) reported approximately €27,580 per km per year for both capital expenditure and operation and maintenance costs across European water utilities [58]. An illustrative cost-feasibility assessment can be constructed for each Pareto-optimal solution based on this. The Dutch drinking water industry's average capital cost component (depreciation plus net interest for distribution mains) at €2088 per km per year for 2023. This figure suggests that, within the Dutch context, capital costs represent a relatively modest share of the total lifecycle cost, with operational expenditure dominating the annual burden. It must be noted, however, that this Dutch capital figure pertains to existing drinking water distribution mains and is not directly transferable to new-build industrial reuse pipelines, where construction complexity, soil conditions, permitting, and subsurface conflicts in an urban brownfield setting such as the Port of Amsterdam are likely to inflate CAPEX considerably. It is therefore used here cautiously as a lower-bound reference point rather than a design-grade estimate.

For Solution 9, the compromise scenario at 14.7 km of pipeline, the annualized lifecycle cost is approximately €405,000 per year based on the €27,580/km/year benchmark [58]. Given that this solution reuses approximately 59.3 m^3/h, equivalent to roughly 519,500 m^3/year under the steady-state assumption, this translates to an infrastructure burden of approximately €0.78/m^3 of water saved. Compared to the current regional drinking water tariff of approximately €1.76/m^3 inclusive of provincial tax and VAT [59], Solution 9 yields an illustrative net saving of approximately €0.98/m^3, implying a positive return on infrastructure investment under current tariff conditions. Applying the Dutch-specific capital decomposition from EBC [58] as a lower bound, the capital-only cost component for Solution 9 would be approximately €30,700 per year, reinforcing that even under conservative CAPEX assumptions the operational savings dominate the cost structure. This cost-per-m^3 framing is consistent with Boysen et al. (2020) [27], who evaluated water reuse economics in a model German industrial park and found that economies of scale reduce unit reuse costs by up to 33% for larger reuse volumes, similarly favors the higher-volume solutions on the Port of Amsterdam Pareto front.

For the maximal Solution 0 at 39.4 km, the annualized lifecycle cost rises to approximately €1.08 million per year, yielding a break-even infrastructure cost of approximately €1.80/m^3 of water saved. This is marginally above the current drinking water tariff, meaning Solution 0 is effectively cost-neutral under present pricing. However, given Amsterdam's projected water scarcity horizon and the regulatory trajectory under the revised Urban Wastewater Treatment Directive (2024/3019), a modest tariff escalation of 15–20% over the infrastructure's operational lifetime would shift Solution 0 from cost-neutral to cost-positive, providing retroactive justification for the higher capital commitment. This sensitivity to tariff trajectory underscores why Solution 0 is most appropriate for stakeholders with long planning horizons and formal water security obligations, rather than for cost-driven near-term investment decisions.

These illustrative calculations suggest that the Pareto front can be meaningfully stratified by financial viability under current conditions. Solutions with annualized infrastructure costs below approximately €1.76/m^3 of saved water, the current tariff threshold. This represents cost-justified investments, placing Solution 9 clearly within the viable range and Solution 0 at the margin. Non-Pareto solutions such as Solution 2, which requires 25.5 km of pipeline to achieve only 44.1 m^3/h freshwater consumption, fall outside this threshold entirely, with an infrastructure cost of approximately €1.36/m^3 against savings of only €0.40/m^3 relative to Solution 9, also confirming their inefficiency from both an infrastructure and financial standpoint.

It must be emphasized that all figures presented here are order-of-magnitude planning estimates based on published benchmarks rather than site-specific engineering quotations. Future work should integrate actual pipe diameter selection based on the WPA-allocated flow volumes, pump energy requirements, and site-specific construction cost data to produce engineering-grade estimates supporting formal investment approval. Incorporating such data would also enable payback period and net present value calculations for individual Pareto-optimal solutions, substantially enhancing the framework's applicability for industrial and municipal decision-makers [58].

Factors such as terrain, construction complexity, and regulatory approvals were not considered in the analysis, meaning that future studies should incorporate these aspects to provide a more accurate understanding of infrastructure costs. Additionally, the single contaminant focus on chloride limits the general applicability of the findings to other industries. Furthermore, the quantitative trade-offs identified in our Pareto front do not represent the general reuse potential of the cluster, as they are strictly constrained by the single-contaminant assumption. Introducing multiple contaminants (e.g., heavy metals, organics) would introduce competing quality thresholds, inevitably reducing the volume of viable cross-industry water exchanges. Expanding the analysis to include multi-contaminant wastewater streams will provide more robust insights into industrial water reuse challenges. To evaluate model robustness in the absence of stochastic variance ranges required for an exhaustive sensitivity analysis, a deterministic stress-test was conducted on the network's liminal capacities regarding both threshold drift and flow variance. A critical analysis of the underlying allocation algorithm reveals the inherent fragility of utilizing high-tolerance steady-state data for long-term infrastructural planning. The Nearest Neighbor Algorithm (NNA) optimizes network efficiency by operating at the absolute margins of the system's mass-balance limits, utilizing convergence tolerances as tight as 10^{-6}. Consequently, the resulting network topologies exhibit severe vulnerability to single-node fluctuations. For instance, the baseline optimization heavily leverages the cluster's largest wastewater producer (yielding 29.14 m^3/h). Should long-term macroeconomic shifts force this single facility to reduce its operational capacity by a highly plausible margin of just 15%, it would induce an immediate cascading hydraulic deficit of approximately 4.3 m^3/h across downstream sinks. From a long-term planning perspective, this quantitative 'brittleness' mandates that municipal authorities cannot design pipeline capacities based solely on optimal WPA flows. Instead, the final engineered network must be oversized with redundant freshwater bypass valves and automated flow-control loops to absorb inter-annual volumetric shocks without starving critical downstream industries. Furthermore, this steady-state assumption obscures risks associated with contaminant drift. In maximizing freshwater displacement, the algorithm dynamically pairs sources and sinks until the maximum allowable contaminant load (C_{in}^{max}) is exactly met, leaving a zero-percent 'quality safety buffer.' If an upstream source experiences a long-term chloride drift of just 50mg/L due to mechanical aging, the downstream match will immediately violate regulatory thresholds, rendering the connecting pipeline legally obsolete. To mitigate this lock-in, future long-term planning must mandate oversized hydraulic capacities and enforce an artificial 'quality safety factor', capping allocations at 80% of a sink's legal tolerance.

While the model is developed using the Port of Amsterdam as a case study, the WPA–GIS integration approach has broader applicability to industrial clusters worldwide. Many industrial zones, such as those in Houston (USA), the Pearl River Delta (China), or Gujarat (India) face similar challenges related to water scarcity, spatial coordination, and regulatory thresholds for water reuse [60–62]. While the integration of WPA and GIS provides a robust framework transferable to global industrial zones, a critical assessment of the model's architecture reveals distinct boundaries for generalization. Because the deterministic model intentionally circumvents the exhaustive data requirements of dynamic stochastic programming, it can be rapidly deployed in data-scarce or emerging industrial zones to establish spatial feasibility bounds and baseline capital expenditures. However, it cannot be generalized as a final operational blueprint for regions dominated by highly volatile

batch processing or competing multi-contaminant synergy. Furthermore, the methodology exhibits strict computational scaling boundaries. The Pareto front extraction deployed in this study utilizes a deterministic, pairwise comparative sorting algorithm. For a mid-sized eco-industrial park (e.g., 17 facilities), this computational complexity is highly efficient. However, when generalizing this methodology to mega-clusters encompassing hundreds or thousands of interconnected nodes, the factorial explosion of potential source-sink iterations renders this exhaustive deterministic sorting computationally prohibitive. Future work should explore the substitution of the NNA heuristic with solver-based optimization methods, particularly for larger industrial clusters where the deterministic exhaustion approach becomes computationally prohibitive. MILP formulations, as demonstrated by Tan et al. (2007) [61] and Alva-Argáez et al. (2007) [32], could be adapted to an industrial cluster and integrate with the GIS routing module to simultaneously optimize water quality matching and pipeline routing within a single mathematical program, potentially identifying Pareto-superior solutions that the greedy NNA misses. Alternatively, population-based metaheuristics such as genetic algorithms or simulated annealing could generate the Pareto front more efficiently for clusters exceeding 50 facilities, where the number of feasible source-sink pairings renders deterministic exhaustion intractable. Critically, any such extension should preserve the GIS road-network routing as a hard constraint on the spatial component, ensuring that the improved allocation logic is matched by equally rigorous spatial feasibility verification.

The methodology's reliance on commonly collected water quality data (e.g., chloride, COD) and the use of open GIS platforms enables transferability across contexts. Specifically, replication of this framework in other regions requires three minimum datasets: (1) Spatial Data: Georeferenced facility locations and a vector-based road network (e.g., OpenStreetMap) for routing; (2) Hydraulic Data: Average volumetric flow rates (m^3/h) for both wastewater generation and process water demand; and (3) Quality Data: Concentration levels (mg/L) of the region's 'limiting contaminant' (e.g., Chloride, COD, Heavy Metals) that drives local regulatory reuse limits. Adaptation to a new cluster then involves three key steps: first, identifying the primary limiting contaminant to define the pinch quality; second, populating the WPA algorithm with local source-sink data to identify valid theoretical matches; and third, executing the GIS routing over the local infrastructure graph to validate spatial feasibility. Furthermore, the modular structure of the model allows adaptation to diverse contaminants, pricing structures, and local reuse guidelines. This generalizability makes the framework suitable not only for water-intensive industries but also for regions aiming to adopt circular water strategies under spatial and economic constraints. Finally, the conversion of annual water usage into a continuous 24/7 hourly flow rate represents a major constraint on the model's reliability. Because real-world industrial clusters operate asynchronously, this steady-state assumption risks overestimating direct reuse capabilities. A primary limitation of the current deterministic model is its reliance on a steady-state, 24/7 constant flow assumption, which inherently masks the asynchronous nature of real-world industrial operations. For instance, a batch wastewater discharge from a chemical plant may not temporally align with the continuous cooling demand of a neighboring power station. To resolve this temporal mismatch, future iterations of this framework must transition from static mass balances to dynamic simulation. Specifically, the integration of Machine Learning (ML) presents a direct pathway to overcoming the current model's static limitations. By training supervised time-series forecasting algorithms (e.g., Random Forest or Long Short-Term Memory networks) on historical Supervisory Control and Data Acquisition (SCADA) datasets, future frameworks can predict exact hourly variances in wastewater generation and process demand [63,64]. In this context, ML is not used for generic network optimization, but specifically for 'predictive buffering.' By forecasting intermittent batch release windows, the system calculates precise hour-by-hour net flows, enabling both the optimal sizing of buffer tanks during the design phase and the dynamic actuation of network valves during real-time operations. This ensures that the spatial topologies and pipeline capacities proposed in our static Pareto front possess the necessary hydraulic resilience to survive peak asynchronous operations without reverting to capital-intensive oversizing. To conceptualize this operational transition, Fig. 6 illustrates the proposed decision-making architecture for the predictive buffering system, detailing the control logic from continuous SCADA ingestion to physical infrastructure actuation.

The implementation of collaborative infrastructure models, where multiple industries share pipelines or storage could lower costs and improve adoption, particularly among SMEs.Integrating real-time data on water demand and contaminant fluctuations could enable more adaptable and robust water management strategies, further supporting

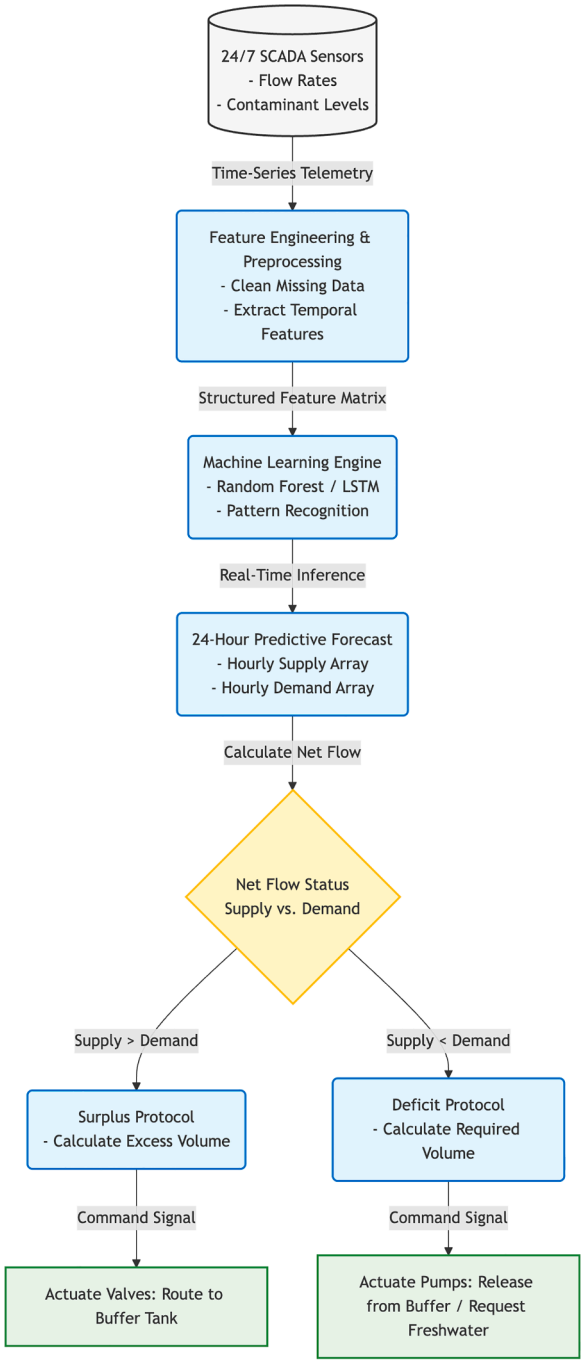


Fig. 6. Proposed decision-making architecture for the ML-driven predictive buffering system.

circular water management. Collaborative frameworks, such as shared infrastructure models and public-private partnerships, can help distribute these costs, making large-scale water reuse more viable for diverse industrial participants.

5. Conclusion

This study developed and applied an integrated Water Pinch Analysis (WPA) and Geographic Information Systems (GIS) framework to optimize cross-industry water reuse within an industrial cluster. Using the Port of Amsterdam as a case study, the model demonstrated that aligning single contaminant-based process integration with spatial routing constraints can significantly reduce freshwater consumption and infrastructure requirements. Crucially, the quantitative results and network configurations derived in this study are explicitly valid only for single-contaminant (chloride) systems, and represent a theoretical upper bound rather than the general, multi-contaminant reuse potential of the cluster. With this boundary explicitly acknowledged, the key contribution of this work is the demonstration that aligning quality-based source-sink matching with spatially constrained pipeline routing can significantly reduce freshwater dependency in an industrial cluster, while providing stakeholders with a structured, reproducible trade-off framework for infrastructure decision-making.

Key findings of this study include:

- Freshwater demand was reduced from approximately 79.2 m^3/h to 10 m^3/h under maximal infrastructure scenarios, highlighting substantial reuse potential.
- GIS integration enabled spatially efficient pipeline routing and informed early-stage infrastructure planning.
- Multi-objective optimization revealed trade-offs between freshwater savings and network complexity, supporting stakeholder decision-making.
- The framework offers a scalable approach to structured reuse planning, particularly relevant for small and mid-sized enterprises lacking centralized reuse infrastructure.

This work addresses a gap in spatial-process integration for industrial water reuse, offering a reproducible method for aligning engineering feasibility with geographic constraints. It supports regional circular economy strategies and provides actionable insights for utilities and planning authorities aiming to reduce potable water use in industrial settings.

Limitations and future work:

- Chloride was selected as the reuse-limiting contaminant; however, because our findings are strictly limited to single-contaminant matching, future models must incorporate multi-contaminant scenarios (e.g., BOD and heavy metals) to determine true operational limits
- The model assumes steady-state 24/7 operation, masking real-world temporal asynchrony such as batch discharges and shift patterns; all freshwater savings and Pareto solutions therefore represent theoretical upper bounds, and future work should incorporate time-step modelling or dynamic programming to improve operational reliability.
- Cost was inferred from spatial distance as a first-order proxy; the pipeline length metric captures infrastructure extent but not construction complexity, pipe diameter, soil conditions, or permitting costs specific to the Port of Amsterdam's urban brownfield context. Inclusion of benchmarked infrastructure and operational costs in future work will enhance economic realism and enable formal payback period calculations.

Overall, this research contributes a flexible planning tool for circular water systems in industrial clusters, with practical implications for infrastructure design and policy development.

Funding

This study was funded by the H2020-AquaSPICE project (EC, CE-SPIRE-07–2020, Horizon 2020). This project has received funding from the European Union's Horizon-2020 research and innovation program under grant agreement No 958,396. The responsibility for the content of this publication lies with the authors. It does not necessarily reflect the opinion of the European Union, and the European Commission is not responsible for any use that may be made of the information contained herein.

Data available statement

The data that support the findings of this study were obtained from Waternet and individual industrial clients. Due to confidentiality agreements and the sensitive nature of industrial data, restrictions apply to their availability. These data were used under license for the present study and cannot be shared publicly. Data may be made available from the authors upon reasonable request and with prior permission from Waternet and/or the respective industrial clients.

Declaration of generative AI usage

During the revision of this work, the author(s) used Grammarly to improve readability. The author(s) reviewed and edited the content and take full responsibility for the publication.

CRediT authorship contribution statement

C.J. Teo: Conceptualization, Methodology, Formal analysis, Investigation, Data curation, Writing – original draft, Writing – review & editing, Visualization. **J. Poinapen:** Conceptualization, Writing – review & editing, Supervision, Funding acquisition. **J.A.M.H. Hofman:** Conceptualization, Methodology, Validation, Resources, Writing – review & editing, Supervision. **T. Wintgens:** Conceptualization, Validation, Resources, Writing – review & editing, Supervision, Funding acquisition.

Declaration of competing interest

The authors declare the following financial interests/personal relationships which may be considered as potential competing interests:

Chuan Jiet Teo reports financial support was provided by European Commission. If there are other authors, they declare that they have no known competing financial interests or personal relationships that could have appeared to influence the work reported in this paper.

Acknowledgement

The authors extend their sincere gratitude to Koen Maathuis, Michael Hessing and Peter Piekema from Waternet, James Hallworth from Port of Amsterdam, Marlies Lambregts from OD NZKG for their assistance in organising and facilitating outreach to industry contacts and also brainstorming on the ideas and methodology.for this work. Special thanks are also due to our colleagues at KWR, including Nienke Koeman-Stein, Julain Muñoz Sierra and Frank Oesterholt, for their valuable expertise and insights, which significantly contributed to the quality and depth of this study.

Appendix

See Table 2

Table 2
Results from iterations of the nearest neighbour algorithm.

Iteration	Number of Unsatisfied Sinks	Total Freshwater Required [m^3/h]
0	0	10.4
1	0	18.1
2	0	44.1
3	0	44.1
4	0	32.6
5	0	55.5
6	0	58.5
7	0	58.5
8	0	58.5
9	0	19.9
10	0	53.3
11	0	79.2

Data availability

Data will be made available on request.

References

[1] S.B. Grant, et al., Taking the "waste" out of "wastewater" for Human water security and ecosystem sustainability, Science 337 (6095) (2012) 681–686, https://doi.org/10.1126/science.1216852.

[2] J.S. Albert, Scientists' warning to humanity on the freshwater biodiversity crisis, Ambio 50 (1) (2021) 85–94, https://doi.org/10.1007/s13280-020-01318-8.

[3] P.H. Gleick, A look at twenty-first century water Resources development, Water. Int. 25 (1) (2000) 127–138, https://doi.org/10.1080/02508060008686804.

[4] X. Ma, X. Xue, A. González-Mejía, J. Garland, J. Cashdollar, Sustainable water systems for the city of tomorrow—a conceptual framework, Sustainability 7 (9) (2015) 12071–12105, https://doi.org/10.3390/su70912071.

[5] C. He, Future global urban water scarcity and potential solutions, Nat. Commun. 12 (1) (2021) 4667, https://doi.org/10.1038/s41467-021-25026-3.

[6] A. Boretti, L. Rosa, Reassessing the projections of the World Water Development Report, NPJ. Clean. Water. 2 (1) (2019), https://doi.org/10.1038/s41545-019-0039-9, 15–15.

[7] B. Baldassarre, M. Schepers, N. Bocken, E. Cuppen, G. Korevaar, G. Calabretta, Industrial Symbiosis: towards a design process for eco-industrial clusters by integrating circular Economy and Industrial Ecology perspectives, J. Clean. Prod. 216 (2019) 446–460, https://doi.org/10.1016/j.jclepro.2019.01.091.

[8] E. Fernandes, R.C. Marques, Review of water reuse from a circular economy perspective, Water 15 (5) (2023) 848, https://doi.org/10.3390/w15050848, 848–848.

[9] C.H Jaynes, Global freshwater demand will exceed supply 40% by 2030, experts warn, World Econ. Forum. (2023).

[10] C.J. Teo, J. Poinapen, J. Hofman, and T. Wintgens, 'Assessing water dependencies and risks in Dutch industries: distribution, consumption and future challenges', 2024, doi: 10.2139/ssrn.4887657.

[11] Y.P. Wang, R. Smith, Wastewater minimisation, Chem. Eng. Sci. 49 (7) (1994) 981–1006, https://doi.org/10.1016/0009-2509(94)80006-5.

[12] M. Al-Otaibi, M. El-Halwagi, Targeting techniques for enhancing process yield, Chem. Eng. Res. Des. 84 (10) (2006) 943–951, https://doi.org/10.1205/cherd.05056.

[13] M.M. El-Halwagi, F. Gabriel, D. Harell, Rigorous graphical targeting for resource conservation via material recycle/reuse networks, Ind. Eng. Chem. Res. 42 (19) (2003) 4319–4328, https://doi.org/10.1021/ie030318a.

[14] S.G. Olesen, G.T. Polley, A simple methodology for the design of water networks handling single contaminants, Chem. Eng. Res. Des. 75 (4) (1997) 420–426, https://doi.org/10.1205/026387697523886.

[15] N. Hallale, A new graphical targeting method for water minimisation, Adv. Environ. Res. 6 (3) (2002) 377–390, https://doi.org/10.1016/S1093-0191(01)00116-2.

[16] J.F.S. Gomes, E.M. Queiroz, F.L.P. Pessoa, Design procedure for water/wastewater minimization: single contaminant, J. Clean. Prod. 15 (5) (2007) 474–485, https://doi.org/10.1016/j.jclepro.2005.11.018.

[17] H. Liu, L. Ren, H. Zhuo, S. Fu, Water footprint and Water pinch analysis in ethanol industrial production for Water management, Water 11 (3) (2019) 518, https://doi.org/10.3390/w11030518, 518–518.

[18] M. Dakwala, B. Mohanty, R. Bhargava, A process integration approach to industrial water conservation: a case study for an Indian starch industry, J. Clean. Prod. 17 (18) (2009) 1654–1662, https://doi.org/10.1016/j.jclepro.2009.08.007.

[19] S. Mohammadnejad, G.R.N. Bidhendi, N. Mehrdadi, Water pinch analysis in oil refinery using regeneration reuse and recycling consideration, Desalination 265 (1–3) (2011) 255–265, https://doi.org/10.1016/J.DESAL.2010.07.059.

[20] A. Alva-Argáez, A.C. Kokossis, R. Smith, The design of water-using systems in petroleum refining using a water-pinch decomposition, Chem. Eng. J. 128 (1) (2007) 33–46, https://doi.org/10.1016/j.cej.2006.10.001.

[21] R.R. Tan, D.K.S. Ng, D.C.Y. Foo, K.B. Aviso, A superstructure model for the synthesis of single-contaminant water networks with partitioning regenerators, Process. Saf. Environ. Prot. 87 (3) (2009) 197–205, https://doi.org/10.1016/j.psep.2009.01.001.

[22] D.C. Faria, M.J. Bagajewicz, Profit-based grassroots design and retrofit of water networks in process plants, Comput. Chem. Eng. 33 (2) (2009) 436–453, https://doi.org/10.1016/j.compchemeng.2008.10.005.

[23] E.M. Lovelady, M.M. El-Halwagi, Design and integration of eco-industrial parks for managing water resources, Environ. Prog. Sustain. Energy 28 (2) (2009) 265–272, https://doi.org/10.1002/ep.10326.

[24] L. Tong, X. Liu, X. Liu, Z. Yuan, Q. Zhang, Life cycle assessment of water reuse systems in an industrial park, J. Environ. Manag. 129 (2013) 471–478, https://doi.org/10.1016/j.jenvman.2013.08.018.

[25] M.S. Taskhiri, R.R. Tan, A.S.F. Chiu, Emergy-based fuzzy optimization approach for water reuse in an eco-industrial park, Resour. Conserv. Recycl. 55 (7) (2011) 730–737, https://doi.org/10.1016/j.resconrec.2011.03.001.

[26] Y. Wen-tao, A case study for engineering design project on the utilization of non-traditional water resources in green industrial parks, South-to-North Water Divers. Water Sci. Technol. (2012).

[27] B. Boysen, J. Cristobal Garcia, J. Hilbig, A. Güldemund, L. Schebek, K.-U. Rudolph, Economic and environmental assessment of water reuse in industrial parks: case study based on a Model Industrial Park, J. Water Reuse Desalin. 10 (2020) 475–489, https://doi.org/10.2166/wrd.2020.034.

[28] G. Skouteris, Water footprint and water pinch analysis techniques for sustainable water management in the brick-manufacturing industry, J. Clean. Prod. 172 (2018) 786–794, https://doi.org/10.1016/J.JCLEPRO.2017.10.213.

[29] A. Esmaeeli, M.H. Sarrafzadeh, Reducing freshwater consumption in pulp and paper industries using pinch analysis and mathematical optimization, J. Water. Process. Eng. 53 (2023) 103646, https://doi.org/10.1016/J.JWPE.2023.103646, 103646–103646.

[30] Z. Ujang, C.L. Wong, Z.A. Manan, Industrial wastewater minimization using water pinch analysis: a case study on an old textile plant, Water. Sci. Technol. 46 (11–12) (2002) 77–84, https://doi.org/10.2166/wst.2002.0720.

[31] E. ODwyer, K. Chen, H. Wang, A. Wang, N. Shah, M. Guo, Optimisation of wastewater treatment strategies in eco-industrial parks: technology, location and transport, Chem. Eng. J. 381 (2020) 122643, https://doi.org/10.1016/j.cej.2019.122643.

[32] A. Alva-Argáez, A.C. Kokossis, R. Smith, The design of water-using systems in petroleum refining using a water-pinch decomposition, Chem. Eng. J. 128 (1) (2007) 33–46, https://doi.org/10.1016/j.cej.2006.10.001.

[33] M. Sorin, S. Bédard, The global pinch point in water reuse networks, Process. Saf. Environ. Prot. 77 (5) (1999) 305–308, https://doi.org/10.1205/095758299530189.

[34] R. Prakash, U.V. Shenoy, Targeting and design of water networks for fixed flowrate and fixed contaminant load operations, Chem. Eng. Sci. 60 (1) (2005) 255–268, https://doi.org/10.1016/j.ces.2004.08.005.

[35] H. Zhou, J. Huang, Y. Yuan, Analysis of the spatial characteristics of the water usage patterns based on ESDA-GIS: an example of Hubei Province, China, Water Resour. Manag. 31 (5) (2017) 1503–1516, https://doi.org/10.1007/S11269-017-1591-Z.

[36] B. Yan, X.R. Su, Y.Y. Chen, Functional structure and data management of Urban Water Supply Network based on GIS, Water Resour Manag 23 (13) (2009) 2633–2653, https://doi.org/10.1007/s11269-009-9400-y.
[37] J. Luettinger, T. Clark, Geographic Information system-based pipeline route selection process, J. Water. Resour. Plan. Manag. 131 (3) (2005) 193–200, https://doi.org/10.1061/(ASCE)0733-9496(2005)131:3(193).
[38] B.A. Gyabeng, Selection of optimum petroleum pipeline routes using A multi-criteria decision analysis and GIS least-cost path approach, Int. J. Sci. Res. Publ. 10 (2020) 572–579, https://doi.org/10.29322/IJSRP.10.06.2020.P10270.
[39] I.A. Rylsky, 'Optimization of pipeline routes using GIS-technologies', pp. 34–40, 2004.
[40] S.A. Taher, J.W. Labadie, Optimal design of water-distribution networks with GIS, J. Water. Resour. Plan. Manag. 122 (4) (1996) 301–311, https://doi.org/10.1061/(ASCE)0733-9496(1996)122:4(301).
[41] N. Gunantara, A review of multi-objective optimization: methods and its applications, Cogent. Eng. 5 (1) (2018) 1502242, https://doi.org/10.1080/23311916.2018.1502242, 1502242–1502242.
[42] M. Chen, R.A. Chowdhury, V. Ramachandran, D.L. Roche, and L. Tong, 'Priority queues and Dijkstra's algorithm', [Online]. Available: https://www3.cs.stonybrook.edu/~rezaul/papers/TR-07-54.pdf.
[43] 'Circulaire economie | Port of Amsterdam', [Online]. Available: https://www.portofamsterdam.com/nl/ontdek/duurzame-haven/circulaire-economie.
[44] A. Fermont, WWTPs as a sustainable freshwater source: a solution for water needs in times of water scarcity, Winnovatie (2023) [Online]. Available, https://www.winnovatie.nl/default.aspx.
[45] Motion by Members Boomsma, Bloemberg-Issa, and Kreuger regarding the drinking water Vision for the future (reducing drinking water use by data centers), Accessed: Sep. 30, https://amsterdam.raadsinformatie.nl/document/11551792/1?connection_type=16&connection_id=757431, 2025.
[46] 'Industrial water supply to the western port area'. Accessed: Sep. 30, 2025. [Online]. Available: https://amsterdam.raadsinformatie.nl/document/11551789/1?connection_type=16&connection_id=757431.
[47] European Parliament and Council of the European Union., 'Directive (EU) 2024/3019 of 27 November 2024 concerning urban wastewater treatment (recast).', 2024. [Online]. Available: https://eur-lex.europa.eu/legal-content/EN/ALL/?uri=CELEX:32024L3019.
[48] J.P. Hoek, H. Fooij, A. Struker, Wastewater as a resource: strategies to recover resources from Amsterdam's wastewater, Resour. Conserv. Recycl. 113 (2016) 53–64, https://doi.org/10.1016/j.resconrec.2016.05.012.
[49] S.V. Valentine, Kalundborg Symbiosis: fostering progressive innovation in environmental networks, J. Clean. Prod. 118 (2016) 65–77, https://doi.org/10.1016/j.jclepro.2016.01.061.
[50] J.J. Klemes, P.S. Varbanov, S.R.W.W. Alwi, Z.A. Manan, Process Integration and Intensification, DE GRUYTER, 2014, https://doi.org/10.1515/9783110306859.
[51] Rijksinstituut voor Volksgezondheid en Milieuhygiëne (RIVM), 'ZZS-emissiedatabase | e-MJV', https://www.e-mjv.nl/zzs, 2024.
[52] X.Y. Fan, Y.P. Li, Z.Y. Liu, C.H. Pan, A new design method for water-using networks of multiple contaminants with the concentration potential concepts, Chem. Eng. Sci. 73 (2012) 345–353, https://doi.org/10.1016/J.CES.2012.02.003.
[53] A. Bhavsar, B. Srinivasan, R. Srinivasan, Freshwater minimization in multistage multiproduct batch processes through intentional waiting, Chem. Eng. Res. Des. 196 (2023) 204–213, https://doi.org/10.1016/j.cherd.2023.06.039.
[54] S.J. Pulluru, R. Akkerman, Analytical framework for planning water reuse in the food industry with application to a cheese production case study, J. Clean. Prod. 423 (2023) 138646, https://doi.org/10.1016/j.jclepro.2023.138646.
[55] D. Kang, K. Lansey, Scenario-based robust optimization of regional water and wastewater infrastructure, J. Water. Resour. Plan. Manag. 139 (3) (2013) 325–338, https://doi.org/10.1061/(ASCE)WR.1943-5452.0000236.
[56] Y.P. Li, G.H. Huang, X. Chen, Multistage scenario-based interval-stochastic programming for planning water resources allocation, Stoch. Environ. Res. Risk Assess. 23 (6) (2009) 781–792, https://doi.org/10.1007/s00477-008-0258-y.
[57] H. Miao, D. Li, Q. Zuo, L. Yu, X. Fei, L. Hao, A scenario-based optimization model for planning sustainable water-resources process management under uncertainty, Processes 7 (5) (2019) 312, https://doi.org/10.3390/pr7050312.
[58] Summary Report IB2023 | European Benchmarking Co-operation, Accessed: Sep. 30, https://www.waterbenchmark.org/content/the-programme-explained_public-report, 2025.
[59] Rates with a water meter, Accessed: Jan. 18, https://www.waternet.nl/en/service-and-contact/tap-water/costs/rates-with-a-water-meter/, 2026.
[60] S. Baccour, et al., Water quality management could halve future water scarcity cost-effectively in the Pearl River Basin, Nat. Commun. 15 (1) (2024) 5669, https://doi.org/10.1038/s41467-024-49929-z.
[61] D. Rich, E. Andiroglu, K. Gallo, S. Ramanathan, A review of water reuse applications and effluent standards in response to water scarcity, Water. Secur. 20 (2023) 100154, https://doi.org/10.1016/j.wasec.2023.100154.
[62] S.M.W. Reddy, et al., Finding solutions to water scarcity: incorporating ecosystem service values into business planning at The Dow Chemical Company's Freeport, TX facility, Ecosyst. Serv. 12 (2015) 94–107, https://doi.org/10.1016/j.ecoser.2014.12.001.
[63] J. Ruan, Y. Cui, Y. Song, Y. Mao, A novel RF-CEEMD-LSTM model for predicting water pollution, Sci. Rep. 13 (2023) 20901, https://doi.org/10.1038/s41598-023-48409-6.
[64] S. Zhang, J. Cao, Y. Gao, F. Sun, Y. Yang, A deep learning algorithm for multi-source data fusion to predict effluent quality of wastewater treatment plant, Toxics 13 (5) (2025) 349, https://doi.org/10.3390/toxics13050349.